Paper:

Design and Testing of a Micro Thermal Sensor for Non-Contact Surface Defect Detection

Yuki Shimizu†, Yuki Matsuno, Yuan-Liu Chen, and Wei Gao

Nano-Metrology and Control Laboratory, Department of Finemechanics, Tohoku University
6-6-1 Aramaki Aza Aoba, Aoba-ku, Sendai, Miyagi 980-8579, Japan
†Corresponding author, E-mail: yuki.shimizu@nano.mech.tohoku.ac.jp
[Received December 28, 2016; accepted February 23, 2017]

This paper presents an experimental study on a new concept of a surface defect detection method, in which surface defects will be detected by monitoring a change in heat flow between a micro thermal sensor and a smoothly-finished measuring surface such as magnetic disks, sapphire substrates and so on. In the proposed method, the micro thermal sensor is designed to detect surface defects without any contacts in between them. Since the change in heat flow across the gap is utilized, the method is expected to find out both the convex and concave defects. Searching for the possibility of the non-contact surface defect detection by the micro thermal sensor, in this paper, a simple heat transfer model is established to estimate the change in heat flow due to the change in gap between the measuring surface and the sensor surface. Some basic experiments are also carried out by using prototype micro thermal sensors, each of which is composed of a pair of electrodes and a thin metal film resistor, fabricated on both the silicon and glass substrates.

Keywords: surface defect detection, micro thermal sensor, heat flow

1. Introduction

Demands on precision industrial components having smoothly-finished surfaces such as silicon wafers, optics and magnetic disks for information storage, are continuously increasing [1, 2]. In the semiconductor industry, one of the most important indexes is a technology node, which represents the smallest size of the fabricated pattern in the products. The technology node of the very large scale integration (VLSI) is predicted to be 10 nm by 2020 [3]. With the continuous shrinkage of the feature size on a wafer surface, the tolerable size of a surface defect is getting smaller and smaller, as well [3]. In the other industries such as data storage [4], smooth surface finishing with less defects are also desired.

In the process of surface defect inspection, at first, defect detection will be carried out, followed by a defect classification by using measuring instruments such as scanning electron microscopes (SEMs) or atomic force microscopes (AFMs). Since the SEMs and AFMs have limited field of view in a high-resolution mode, existences of surface defects need to be found out by a highly-sensitive detection method in advance of the defect classification. One of another requirements for the defect detection is that surface defects are preferred to be detected in a non-destructive way regarding the following defect classification. For the defect detection, optical methods have often been used so far [5, 6]. A laser scattering method, which is one of the optical methods, has a high sensitivity and can detect defects with the size of several-ten nm. However, it becomes more difficult for the method to detect defects when the defect size gets smaller and smaller, since the intensity of scattered light becomes too weak due to the Rayleigh scattering limitation [7]. It is therefore desired to develop a new detection method that can overcome the limitation of the laser scattering method, and a lot of efforts has been made so far [8–10].

In responding to the background described above, a new concept for the surface defect detection employing a micro thermal sensor has been proposed [11]. The proposed method has been designed in such a way that the thermal sensor scans over a measuring surface while keeping a constant gap between them, and finds out the existence of defect by detecting heat generated in the contact in between them. Some basic experiments have shown that the possibility of the micro thermal sensor detecting a contact with an object with the size of several-ten nm [12, 13]. However, as can be expected, this strategy could give damage to both the defects and the sensor surface. Another drawback of the strategy is that defects with concave shape cannot be detected.

To overcome the drawbacks of the above mentioned method, a new strategy for surface defect detection, in which heat flow in between the sensor surface and a measuring surface is utilized to detect surface defects, is proposed in this paper. To verify the possibility of the proposed method, theoretical calculation is carried out based on a simple heat transfer model simulating the interface between the micro thermal sensor and a measuring surface. In addition, prototype micro thermal sensors are fabricated, and some basic experiments are also carried out.

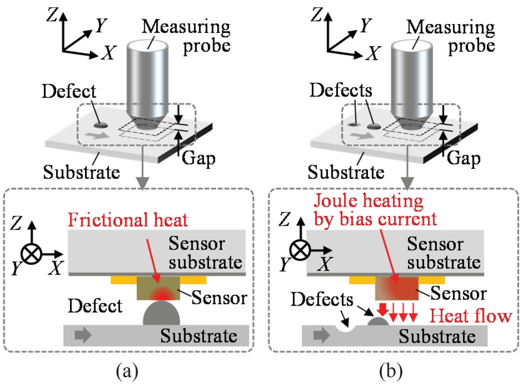

Fig. 1. A schematic of the defect detection by the micro thermal sensor; (a) the previously proposed method relying on contact detection [12], (b) a method proposed in this paper.

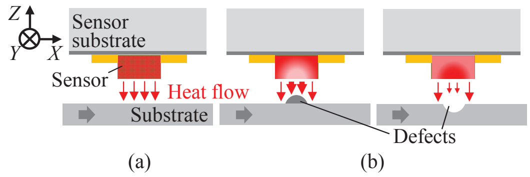

Fig. 2. Expected behavior of the heat flow at the gap between the sensor and substrate surfaces; (a) in thermodynamic equilibrium, (b) in the case of passing over surface defects.

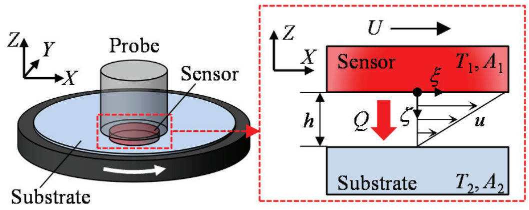

Fig. 3. A heat transfer model at the sensor-substrate gap.

2. Non-Contact Surface Defect Detection

2.1. Principle of the Proposed Method

A schematic of the defect detection method previously proposed by the authors is shown in **Fig. 1(a)** [12]. In the method, a micro-sized thin metal film, which experiences a change in electrical resistance with the deviation of its temperature, is employed as the micro thermal sensor. In this paper, as shown in **Fig. 1(b)**, a major modification is made in the concept for the defect detection. One of the major differences in the new method is that the sensor detects a change in heat flow between the sensor surface and the measuring surface, rather than detecting the heat generated in the contact between the sensor surface and a defect on a measuring surface. In the same manner as the previous method, a gap is placed between the sensor surface and a measuring surface arranged in parallel with each other, while a relative motion is given in between them. Since the sensor temperature becomes higher than that of the surroundings due to the Joule heating by the applied bias voltage, heat flows across the gap. As long as the gap is kept constant as shown in **Fig. 2(a)**, the system is in thermodynamic equilibrium, and the sensor temperature will be kept constant, as well. However, when the sensor scans over a defect, the rate of heat flow deviates with the change in gap, resulting in the change in sensor temperature as shown in **Fig. 2(b)**. In the case of protruded defect, the heat flows faster since the gap becomes smaller, resulting in the decrease in the sensor temperature. On the contrary, when the sensor scans over a recessed defect, the heat flows slower, resulting in the increase of the sensor temperature. By detecting the change in electrical resistance of the sensor due to the deviation of its temperature, both the recessed and protruded defects are expected to be detected without any physical contacts between the sensor and the defects.

It should be noted that the proposed concept is different from the scanning thermal microscope (SThM) [14, 15] mainly designed to investigate the thermal property of the measuring target. Its field of view is typically limited to be smaller than 100 μm$\times$100 μm, and is therefore not suitable for surface defect detection. In addition, although similar thermal sensors utilized for displacement measurement can be found in literatures [16, 17], the micro thermal sensor employed in this paper is different in its usage and its apparatus fabricated on a substrate in a micrometric size. Furthermore, in the proposed method, the gap to be set between the sensor and a measuring surface is on the order of sub-micrometer, and is quite smaller than that in the similar thermal sensors [17].

2.2. Theoretical Calculation on the Heat Flow

The rate of heat flow across the gap is estimated based on a simplified heat transfer model, a schematic of which is shown in **Fig. 3**. In the model, the sensor surface and a measuring surface are treated as flat plates arranged in parallel with each other, while a constant relative velocity U is applied in between them. Due to the Joule heating, the temperature of the sensor is higher than that of the surroundings, and depends on the heat balance in between them. In the proposed defect detection method, the gap h between the sensor and the measuring surface is kept constant; in this case, the sensor is in thermodynamic equilibrium and thus the sensor temperature is constant. However, when a defect exists in the gap, the sensor is no longer in thermodynamic equilibrium, and the sensor temperature will be changed.

In this paper, as the first step of the investigation on the heat flow at the gap, the change in heat flow by the defect is expressed as the variation of gap h. Both the sensor and the measuring substrate are assumed to have uniform temperature distribution T_1 and T_2, respectively. In the model, laminar flow of viscous fluid is assumed across the gap since the defect detection will be carried out by scanning the sensor over the measuring surface with a constant gap h and the constant relative velocity U. By including a mean free path λ, the energy equation at the gap can be expressed as follows [18, 19]:

$$\rho C_P u \frac{\partial T}{\partial x} + \rho C_P v \frac{\partial T}{\partial y} - u \frac{\partial p}{\partial x} - v \frac{\partial p}{\partial y}$$

$$= k\frac{\partial^2 T}{\partial z^2} + \mu\left\{\left(\frac{\partial u}{\partial x}\right)^2 + \left(\frac{\partial v}{\partial y}\right)^2\right\} \quad . \; . \; . \; . \quad (1)$$

where the parameters ρ, C_P, p, k, μ, and T are the density, the specific heat at constant pressure, the pressure, the thermal conductivity, the viscosity, and the temperature of the air, respectively. The parameters u and v are the velocities of sensor along the X- and Y-directions, respectively, with respect to the measuring surface given as follows:

$$u = U\left(1 - \frac{z + a\lambda}{h + 2a\lambda}\right), \quad v = 0 \quad . \; . \; . \; . \; . \; . \quad (2)$$

where a is the constant related to the momentum accommodation coefficient [18]. By including the Navier–Stokes equations shown in Eq. (3), Eq. (1) can be rewritten as Eq. (4):

$$\frac{\partial p}{\partial x} = \mu\frac{\partial^2 u}{\partial z^2}, \quad \frac{\partial p}{\partial y} = \mu\frac{\partial^2 v}{\partial z^2}, \quad \frac{\partial p}{\partial z} = 0 \quad . \; . \; . \quad (3)$$

$$\rho C_P u\frac{\partial T}{\partial x} + \rho C_P v\frac{\partial T}{\partial y}$$
$$= k\frac{\partial^2 T}{\partial z^2} + \mu\left[\left(\frac{\partial u}{\partial z}\right)^2 + \left(\frac{\partial v}{\partial z}\right)^2\right] \quad . \; . \; . \; . \; . \quad (4)$$

Now the influence of last term in Eq. (4) is negligibly small. By applying the boundary conditions described as Eq. (5), the sensor temperature T at $x = 0$ can be derived as Eq. (6):

$$T(0) = T_1 + b\lambda\left.\frac{\partial T}{\partial z}\right|_{z=0}, T(h) = T_2 - b\lambda\left.\frac{\partial T}{\partial z}\right|_{z=h} \quad (5)$$

$$T(z) = \frac{T_2 - T_1}{h + 2b\lambda}z + T_1 + b\lambda\left(\frac{T_2 - T_1}{h + 2b\lambda}\right) \quad . \; . \; . \quad (6)$$

where the parameter b can be calculated as follows:

$$b = \frac{2(2 - \sigma_T)\gamma}{\sigma_T(\gamma + 1)Pr} \quad . \; . \; . \; . \; . \; . \; . \; . \; . \; . \; . \; . \quad (7)$$

In these equations, the parameters γ, σ_T, and Pr are the ratio of specific heat, the thermal accommodation coefficient, and the Prandtl number, respectively [18]. From Eq. (6), the heat flux q across the gap h can be calculated as follows:

$$q = -k\frac{\partial T}{\partial z} = -k\frac{T_2 - T_1}{h + 2b\lambda} \quad . \; . \; . \; . \; . \; . \; . \; . \quad (8)$$

The rate of heat flow Q from the sensor surface to the measuring surface can therefore be expressed as follows:

$$Q = Aq = -kA\frac{T_2 - T_1}{h + 2b\lambda} \quad . \; . \; . \; . \; . \; . \; . \; . \; . \quad (9)$$

where A is the effective area of sensor surface. **Fig. 4** shows the calculated rate of heat flow as a function of the gap h. In the calculation, the parameters summarized in **Table 1** are applied to Eq. (9). Q is also calculated for the case with the sphere-shaped substrate surface having the tip radius of 20 μm, on the assumption that Eq. (9) is

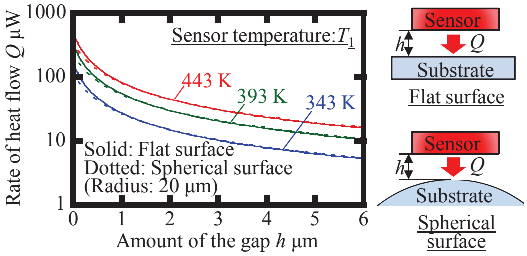

Fig. 4. Estimated rate of heat flow at the gap.

Table 1. Parameters for estimating the rate of heat flow.

Parameter	Symbol	Value	Unit
Temperature of the measuring surface	T_2	293	K
Thermal accommodation coefficient	σ_T	0.80	–
Prandtl number	Pr	0.719	–
Ratio of specific heat	γ	1.4	–
Thermal conductivity	k	2.76×10^{-2}	$\mathrm{Wm^{-1}K^{-1}}$
Mean free path	λ	4.0×10^{-8}	m
Relative velocity	U	5.0×10^{-5}	m/s
Effective area of sensor surface	A	2.5×10^{-11}	$\mathrm{m^2}$

also valid for the case. As can be seen in the figure, Q increases with the decrease of gap h, and is on the order of several-ten μW when h is set to be smaller than 3 μm. By employing the thermal sensor whose sensitivity is high enough to detect the change in rate of heat flow on the order of microwatts or better, the existence of a defect at the gap is expected to be detected. It should be noted that further detailed investigation is required by including the influence of temperature distribution on the sensor surface, while considering the size of a defect.

3. Basic Experiments

To confirm the possibility of detecting a change in the rate of heat flow across the gap by the micro thermal sensor, some basic experiments were carried out. **Fig. 5** shows a schematic of the developed setup for the basic experiments. The employed micro thermal sensor was composed of a thin film chromium, which acted as a temperature-sensitive resistor, and a pair of electrodes [12]. All the sensor structures were prepared on a silicon substrate having an insulation layer (SiO_2) on its top surface. The fabricated micro thermal sensor was mounted on X-, Y-, and Z-piezoelectric (PZT) stages having a positioning resolution of 1 nm along each axis. A displacement sensor was embedded to each of the PZT stage. The micro thermal sensor was integrated into a bridge circuit to monitor the change in its electrical resistance. To simulate the gap between the sensor surface and a measuring surface, in this study, a micro-probe [20] with a tip radius of 25 μm was employed. In the experiments, the sensor surface was firstly brought into contact with the probe tip. The sensor surface was then re-

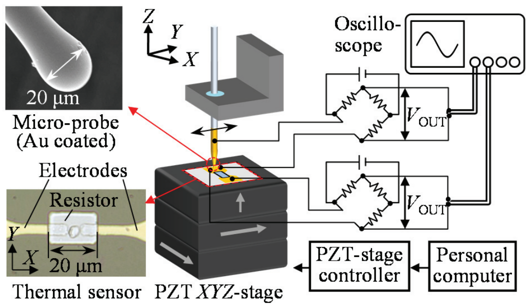

Fig. 5. Schematic of the experimental setup.

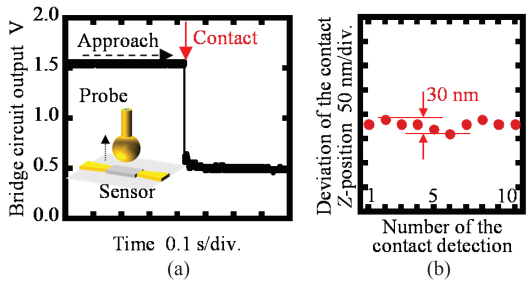

Fig. 6. Contact detection by the Au-coated micro-probe; (a) typical variation of the bridge circuit output at the contact detection, (b) repeatability of the contact detection.

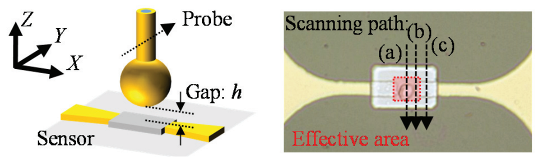

Fig. 7. Micro-probe made to scan over the sensor surface.

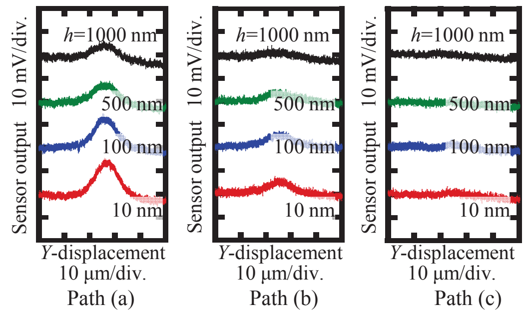

Fig. 8. Variation of the output signal from the sensor when the micro-probe scanned over the sensor surface along the paths (a), (b), and (c) shown in **Fig. 7.**

tracted back from the contact point by the Z-PZT stage. By referring the change in the sensor position along the Z-direction, which could be detected by the displacement sensor in the Z-PZT stage, the amount of the gap h could be assured. To detect the contact between the sensor surface and the probe tip, the micro-probe was sputtered with gold, and was wired to another bridge circuit. **Fig. 6(a)** shows a typical bridge circuit output at the contact detection. The sensor was made to approach the probe tip with a step of 10 nm along the Z-direction. As can be seen in the figure, the contact was successfully detected by the developed system. Ten repeated measurements were carried out. The peak-to-valley repeatability in the detected Z-directional sensor displacement at the contact was 30 nm.

Following the verification of the repeatability of contact detection, another experiment was carried out. **Fig. 7** shows a schematic of the experiment. After adjusting the gap h between the sensor surface and the tip of the micro-probe, the sensor was moved along the Y-direction while being kept stationary along the X- and Z-directions so that the micro-probe could scan over the sensor surface. Three scanning paths (a), (b), and (c) in the figure were chosen to observe the variation of sensor output. **Fig. 8** shows the results. In the experiment, the amount of the gap h was set to be 1000 nm, 500 nm, 100 nm, and 10 nm. In particular, attention was paid to carry out the scan immediately after setting the gap h in the case of $h = 10$ nm. As can be seen in the figure, larger amplitude of the output signal was observed when the probe was closer to the center of the effective area on the sensor surface. In addition, the change in sensor output became larger with the decrease of the gap h. The sensor could even sense the probe scanning with the gap of 1000 nm when the probe scanned over the center of the effective area. These experimental results verified that the developed micro thermal sensor could detect an object passing over its surface by detecting the change in its electrical resistance induced by the change in the rate of heat flow across the gap.

4. Detection of the Periodic Patterns

The experiments were then extended to detect periodic micro patterns. Regarding the application of the proposed method to carry out surface defect detection over a large surface area, the sensor is expected to be held above the sliding/rotating measuring surface, while keeping a certain amount of gap in between them. However, it was difficult for the previously fabricated thermal sensors to be placed above the measuring surface, since wiring points on the electrodes were placed on the same surface as the sensor element and were obstacles to making the effective area of the sensor surface to approach the measuring surface. To solve this problem, major modifications were made in the newly developed thermal sensor, a schematic of which is shown in **Fig. 9(a)**. The first modification was that one of the pairs of opposite sides of the upper face of the sensor substrate was chamfered so that the wiring points on the electrodes could be recessed from the top surface of the thermal sensor. The second modification was that a glass plate was employed as the sensor substrate instead of the silicon wafer so that the gap between the sensor surface and the measuring surface could be measured by using optical instruments. It should be noted that the developments of the optical instruments will be carried out as future work. As can be seen in the figure, the thermal sensor was successfully fabricated even on the glass substrate by using the same fabrication process as the silicon wafer. **Fig. 9(b)** shows the comparison of the sensor sensitivity. In the same manner as the pre-

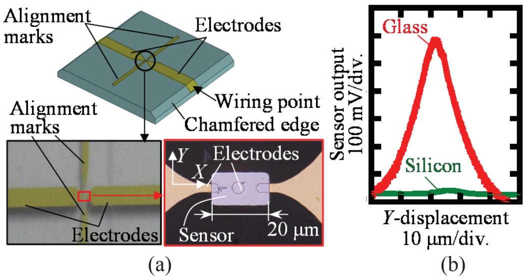

Fig. 9. Thermal sensor fabricated on a glass substrate; (a) photograph of the fabricated sensor, (b) comparison of the sensor sensitivity.

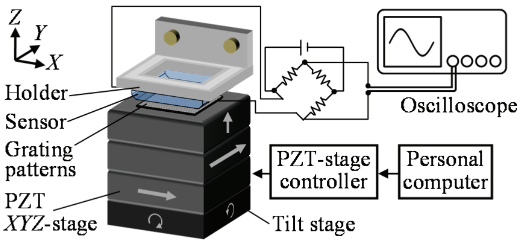

Fig. 10. Experimental setup for detecting grating patterns.

vious experiment, the micro-probe was made to scan over the thermal sensor fabricated on the glass substrate, while monitoring the variation of output signal from the sensor. As can be seen in the figure, the amplitude of the output signal became large. Since the thermal conductivity of the glass was far lower than that of the silicon wafer, the sensor temperature was increased even the same level of bias voltage was applied, resulting in the increase of rate of heat flow across the gap and the improvement of the sensor sensitivity.

Figure 10 shows a schematic of the developed experimental setup, in which the newly fabricated thermal sensor was employed to detect grating patterns prepared on a silicon wafer. The thermal sensor was mounted in a sensor holder, which was held stationary in the setup. The grating, which was a measuring target of the experiments, was mounted on a multi-axis stage system composed of X-, Y-, and Z-PZT stages and a two-dimensional tilt stage. The tilt stage was employed so that the grating substrate could be aligned to be parallel with respect to the sensor surface. In the same manner as the experiments described in the previous section, the micro thermal sensor was integrated into the bridge circuit. **Fig. 11** shows a closed up image of the gap between the sensor surface and the grating surface. In the experiments, the sensor was held stationary, while the grating was moved along the X-direction by using the X-PZT stage. Due to the influence of the grating tilts with respect to the sensor surface, it was difficult to precisely control the amount of the gap h in between them. The gap h was therefore coarsely adjusted to be approximately 2 μm. As the grating patterns, three types of developed line photoresist patterns, the parameters of which are summarized in **Table 2**, were employed. **Fig. 12** shows the variation of the output signal from the thermal sensor observed with the grating patterns of types (a), (b),

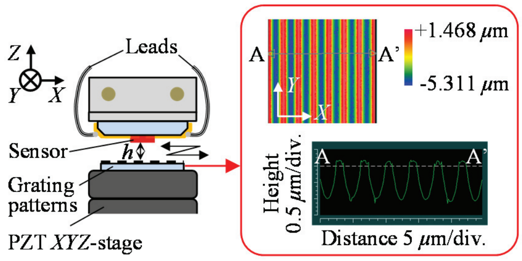

Fig. 11. Schematic of the sensor-measuring surface interface.

Table 2. Grating patterns employed in the experiments.

Type of grating	Period [μm]	Width [μm]	Height [μm]
(a)	15	7	3.2
(b)	20	10	2.2
(c)	30	15	4.0

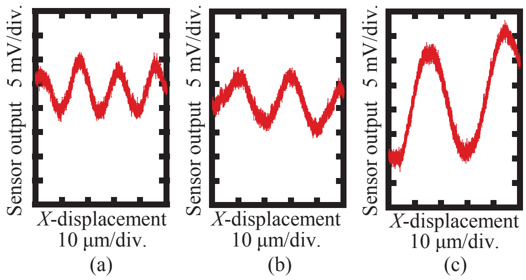

Fig. 12. Observed output signals from the sensor when scanned over the gratings (a), (b), and (c) in **Table 2**.

and (c) in **Table 2**. It should be noted that linear components in the output signals, which were due to the grating tilts with respect to the sensor surface, were eliminated in the figure. In each case, variation of the output signal, whose period well agreed with that of the measured grating patterns, was clearly observed. From these results, it was verified that the developed thermal sensor could detect micro-pattern structures by detecting the change in its electrical resistance, which was induced by the change in rate of heat flow at the gap between the sensor surface and the measuring surface. Meanwhile, the amplitudes of output signals observed in **Figs. 12(a)**, **(b)** and **(c)** did not agree with the heights of grating patterns shown in **Table 2**. One of the main reasons of this discrepancy was considered to be due to the poor tilt angle adjustment of the sensor with respect to the grating surface. In addition, the height profiles of the grating patterns having rounded edges on the top surfaces could have influenced the sensor outputs.

It should be noted that, in this paper, efforts have been made to search for the possibility of detecting micro objects on a measuring surface in a non-contact manner by using the developed micro thermal sensor. For the achievement of high resolution surface defect detection, it is necessary to establish methods for controlling the amount of the gap and the tilts between the sensor and a measuring surface, which will be carried out as future work.

5. Conclusions

A new concept of a surface defect detection method, in which a change in heat flow between a micro thermal sensor and a measuring surface is utilized to find out existences of surface defects, has been proposed. A simple heat transfer model simulating the sensor-measuring surface interface has been established to estimate the rate of heat flow in between them, and it has been revealed that the rate of heat flow on the order of several-ten microwatts detectable by using the developed micro thermal sensor can be expected when the gap is set to be smaller than a few micrometers. To search for the possibility of the micro thermal sensor for detecting an object in a non-contact apparatus, some basic experiments have been carried out. Experimental results have confirmed that the developed sensor can sense an object on a measuring surface by detecting the change in its electrical resistance induced by the change in the rate of heat flow. Furthermore, line patterns with micrometric periods have also successfully been detected by using the sensor fabricated on a glass substrate.

Acknowledgements

This research is supported by Japan Society for the Promotion of Science (JSPS) Grant Number 15H03907.

References:

[1] E. Brinksmeier et al., "Ultra-precision grinding," CIRP Ann. Manuf. Techn., Vol.59, No.2, pp. 652-671, 2010.

[2] B. Marchon and T. Olson, "Magnetic spacing trends: From LMR to PMR and beyond," IEEE Trans. Magn., Vol.45, pp. 3608-3611, 2009.

[3] 2015 Int. Technology Roadmap for Semiconductors, http://www.semiconductors.org/ [accessed December 24, 2016]

[4] A. N. Murthy et al., "Thermal fly-height controlled glide for disk defect detection and defect size estimation for hard disk drives," Microsyst. Technol., Vol.20, pp. 1523-1527, 2014.

[5] P. M. Lonardo, "Surface Characterization and Defect Detection by Analysis of Images Obtained with Coherent Light," CIRP Ann. Manuf. Techn., Vol.40, No.1, pp. 541-544, 1991.

[6] K. Takami, "Defect inspection of wafers by laser scattering," Mat. Sci. Eng. B-Solid, Vol.44, pp. 181-187, 1997.

[7] A. T. Young, "Rayleigh scattering," Appl. Opt., Vol.20, No.4, pp. 533-535, 1981.

[8] D. Meshulach et al., "Advanced lithography: wafer defect scattering analysis at DUV," Proc. of SPIE, Vol.7638, 76380K(10pp), 2010.

[9] R. Attota and R. Silver, "Nanometrology using a through-focus scanning optical microscopy method," Meas. Sci. Technol., Vol.22, 024002(10pp), 2011.

[10] S. Takahashi et al., "Super resolution optical measurements of nanodefects on Si wafer surface using infrared standing evanescent wave," CIRP Ann. Manuf. Techn., Vol.60, pp. 523-526, 2011.

[11] Y. Shimizu et al., "Feasibility study on the concept of thermal contact sensor for nanometre-level defect inspections on smooth surfaces," Meas. Sci. Technol., Vol.25, 064006(11pp), 2014.

[12] Y. Shimizu, Y. Ohba, and W. Gao, "Investigation on Sensitivity of a Contact-Type Thermal Sensor for Surface Defect Inspections," Int. J. Automation Technol., Vol.9, No.3, pp. 291-296, 2015.

[13] Y. Shimizu et al., "Nano-Scale Defect Mapping on a Magnetic Disk Surface Using a Contact Sensor," IEEE Trans. Magn. 47, pp. 3426-3432, 2011.

[14] J. Martinek et al., "Thermal conductivity analysis of delaminated thin films by scanning thermal microscopy," Measurement Science and Technology, Vol.25, 044022(7pp), 2014.

[15] S. Gomes et al., "Characterization of the thermal conductivity of insulating thin films by scanning thermal microscopy," Microelectr. J., Vol.44, pp. 1029-1034, 2013.

[16] M. A. Lantz et al., "A micromechanical thermal displacement sensor with nanometre resolution," Nanotechnology, Vol.16, pp. 1089-94, 2005.

[17] B. Krijnen et al., "A single-mask thermal displacement sensor in MEMS," J. Micromech. Microeng., Vol.21, 074007(12pp), 2011.

[18] S. Zhang and D. B. Bogy, "A heat model for thermal fluctuations in a thin slider/disk air bearing," Int. J. Heat Mass Transfer, Vol.42, pp. 1791-1800, 1999.

[19] F. Kreith, R. M. Manglik, and M. S. Bohn, "Principle of Heat Transfer," 7th ed., SI ed., Cengage learning, 2011.

[20] W. Gao, "Precision Nanometrology: Sensors and Measuring Systems for Nanomanufacturing," Springer, 2010.

Name:
Yuki Shimizu

Affiliation:
Associate Professor, Department of Finemechanics, Tohoku University

Address:
6-6-1 Aramaki Aza Aoba, Aoba-ku, Sendai, Miyagi 980-8579, Japan

Selected Publications:
• "Nano-scale defect mapping on a magnetic disk surface using contact sensor," IEEE Trans. Magn., Vol.47, pp. 3426-3432, 2011.

Name:
Yuki Matsuno

Affiliation:
Associate Professor, Department of Finemechanics, Tohoku University

Address:
6-6-1 Aramaki Aza Aoba, Aoba-ku, Sendai, Miyagi 980-8579, Japan

Name:
Yuan-Liu Chen

Affiliation:
Associate Professor, Department of Finemechanics, Tohoku University

Address:
6-6-1 Aramaki Aza Aoba, Aoba-ku, Sendai, Miyagi 980-8579, Japan

Selected Publications:
• "An in-process measurement method for repair of defective microstructures by using a fast tool servo with a force sensor," Precision Engineering, Vol.39, pp. 134-142, 2015.

Name:
Wei Gao

Affiliation:
Professor, Department of Finemechanics, Tohoku University

Address:
6-6-1 Aramaki Aza Aoba, Aoba-ku, Sendai, Miyagi 980-8579, Japan

Selected Publications:
• Precision Nanometrology: Sensors and Measuring Systems for Nanomanufacturing, ISBN 978-1-84996-253-7, Springer, 2010.